LAWRENCE
LIVERMORE
NATIONAL
LABORATORY

UCRL-JRNL-232907

Temperature dependence of protein hydration hydrodynamics by molecular dynamics simulations.

Edmond Y. Lau, V. V. Krishnan

July 20, 2007

Biophysical Chemistry

Temperature dependence of protein hydration hydrodynamics by molecular dynamics simulations.

Edmond Y. Lau

Biology & Biotechnology Division, Lawrence Livermore National Laboratory, Livermore,

California

V.V. Krishnan

Department of Chemistry, California State University Fresno, Fresno, California
Department of Applied Science and Center for Comparative Medicine, University of California Davis, Davis, California

Corresponding Author
V.V. Krishnan
vvkrishnan@ucdavis.edu / krish@csufresno.edu

Running title: Temperature dependence of protein hydration dynamics

Manuscript information: Figures (4); Tables (4); Abstract (135 words); Total number of words (4,932) excluding references.

Key Words: MD, Molecular dynamics; Hydration, Hydrodynamics, water, protein, diffusion.

Abstract

The dynamics of water molecules near the protein surface are different from those of bulk water and influence the structure and dynamics of the protein itself. To elucidate the temperature dependence hydration dynamics of water molecules, we present results from the molecular dynamic simulation of the water molecules surrounding two proteins (Carboxypeptidase inhibitor and Ovomucoid) at seven different temperatures (T=273 to 303 K, in increments of 5 K). Translational diffusion coefficients of the surface water and bulk water molecules were estimated from 2 ns molecular dynamics simulation trajectories. Temperature dependence of the estimated bulk water diffusion closely reflects the experimental values, while hydration water diffusion is retarded significantly due to the protein. Protein surface induced scaling of translational dynamics of the hydration waters is uniform over the temperature range studied, suggesting the importance protein-water interactions.

Introduction

Water plays a crucial role in determining the structure, dynamics, and function of proteins and other biological macromolecules. It is implicated in the folding, unfolding, and stabilization of protein three-dimensional structure, as well as in the internal dynamics and function (1-9). Protein-water interaction affects the water molecules near the protein, leading to a behavior that is very different from bulk water (10-12). These water molecules, widely known as interfacial or surface water molecules can be considered in general terms as hydration water, and a better understanding of their properties is necessary to gain insight into various biological mechanisms of protein function (13-15). The dynamics and other properties of water near protein surface has been elucidated by a multitude of experimental methods; these include calorimetry, thermodynamic measurements (16), nuclear magnetic resonance (NMR) analysis (17-19), X-ray and neutron small-angle scattering (20), high resolution X-ray crystallography (21-25), and high resolution neutron crystallography (26,27). All these studies showed that water molecules on the protein surface mainly occupy well-defined hydration sites (time and space averaged water molecule position), providing stability to the protein structure and mediating interactions with other components of the cell.

There is increasing evidence over the past decade and in particular in the last four years that hydration water molecules play a synergetic role in protein structure, dynamics, as well as function (6-8). Although experimental measurements indirectly show that, the physical properties of hydration water molecules are different from that of bulk water, molecular dynamics (MD) simulations are capable of providing information on the time and the geometric scale commensurate with the diffusive motions of individual water molecules responsible. Several MD studies have been performed on protein solution or protein crystals and provide a wide range of observations and at times

contradictory (28-30). Lack of consistent experimental and computational investigations on model protein-water systems make it difficult to compare the structural and dynamical results across the different studies. In addition, most of the calculations have been restricted to either short simulation length or to a single temperature. As a first step towards generating a consistent set of data, we present a molecular dynamic study of water molecules in two protein systems, as a function of temperature.

Molecular dynamics simulation of protein-water systems of two different model proteins, Carboxypeptidase inhibitor (CPI) and Ovomucoid (OVO), in explicit water as a function of temperature from 273 K to 303 K is presented. The choice of the proteins was decided by their size that allows sampling of the water dynamics that are computationally inexpensive and at the same time provide the necessary features to generalize the results. CPI is a small protein of 39 residues (MW=4.36 kD) with the three-dimensional structure well stabilized by intramolecular disulphide bonds (31). OVO is a medium sized protein of 56 residues long (MW=6.04 kD). Analysis of the molecular dynamics simulation trajectories of the water molecules provides characteristic differences in the dynamic behavior between the bulk and surface water molecules. In particular, we find that our results are similar to the trend suggested by the modified Stokes-Einstein equation for biomolecular hydration (32). These results perhaps provide a first set of consistent simulation data to understand the temperature dependence of the translational dynamics of water molecules.

Results

Temperature dependence of radial distribution functions

The structural organization of water at the protein interface is generally described by protein-water radial distribution functions that represent the relative probability of finding any solvent molecule at a distance '*r*' from a specific solute atom (33,34). The radial distribution function (RDF) of the water molecules around the proteins has been calculated for both polar and nonpolar residues separately. **Figure 1** shows the shows plots of the radial distribution function of the backbone carbons (α and carbonyl), and nitrogen to the water oxygen at three representative temperatures (at 273, 288 and 303 K) for the protein CPI with the left panels (a, c and e) for the nonpolar residues and the right panels (b, d and f) for the polar residues. Similarly, **Figure 2** shows the results for the protein Ovomucoid. The plot of the radial distribution function is used to evaluate the quality of the dynamic trajectories. All the distribution functions in figures 1 and 2 show the characteristic peaks, with the first one centered around 2-3 Å, arising from the strong interaction of the water oxygen with hydrogen bond acceptor groups of the protein surface, and the second peak at a location farther from the first one (4-5 Å) due to interaction between the water oxygen and nonpolar heavy atoms of the proteins (33,35). Figures 1 and 2 also show the bulk limit of the radial distribution is generally reached for distances greater than 8 Å from the protein surface, supporting the lack of persistence of the structural organization of bulk water. For both proteins, the first peak for solvent exposed residues' the C, N and O distribution occurs at 3.8, 3.0 and 2.8 Å, respectively and the distribution functions at 273 K have slightly higher values than the values at the higher temperatures.

Translational dynamics of bulk and protein-hydration waters

The combination of Einstein's fluctuation dissipation theorem (36) and the macroscopic continuum hydrodynamics (37) for the friction coefficients of a sphere of radius '*a*' undergoing steady state translational diffusion yields the Stokes-Einstein equation,

$$D_S = \frac{k_B T}{6\pi\eta a} \qquad [1]$$

where k_B is Boltzmann's constant (1.3806 $\times 10^{-23}$ $m^2 kgs^{-2}K^{-1}$), T is the temperature in K, and η is water viscosity (Nsm^{-2}). ,The viscosity of water, as a function of temperature, follows the definition of a glass-forming liquid (38) and at temperatures above 242K, it follows an empirical Vogel-Tamman-Fulcher (VTF)-type relationship ($\eta = A\exp(-B/(T-T_0))$, where A, B, and T_0 are constants (38). Diffusion constants of water have been measured using nuclear magnetic resonance (NMR) pulsed-field-gradient (PFG) methods (39) and these measurements also followed VTF-type relation ship ($D_S = A\exp(-B/(T-T_0))$, with constants A = 4.00 × 10^{-8} m^2 s^{-1}, B = 371 K^{-1} and T_0 = 169.7 K. These numbers are close to the one derived by Miller (38). Therefore, a plot of D_s versus T/η is expected to be linear and can be used as a quantitative measure of the change in the diffusion constant as a function of temperature. **Figure 3** shows plots of the diffusion coefficient as a function of T/η for CPI (Fig 3a) and Ovomucoid (Fig. 3b). Experimentally measured bulk water diffusion coefficients (39) are shown as open circles in both Figures 3a and 3b. Diffusion constant of the bulk water from the molecular dynamics simulations are shown as filled circles. Hydration (surface) water molecules calculated using a cutoff at 3.4 Å and 5.0 Å are shown by triangles and triangles and squares, respectively. The bulk water diffusion constants (filled circles in Fig 3) are

calculated independently for CPI and Ovomucoid systems. The straight lines thorough the points represent corresponding linear fit and the dashed lines correspond to the respective 95% confidence limits. The literature values for η follow the well defined empirical relations for pure water (39) and it is assumed that the bulk viscosity is not altered at low protein concentration.

Table 1 summarizes translational diffusion constants for bulk and hydration water from the CPI and Ovomucoid simulations and the respective experimental bulk water values. Table 1 also lists the reduction in the translational diffusion constant of the hydration water in percentage for each temperature with respect to the corresponding bulk water diffusion coefficients. It is evident from Fig.3 and from Table 1 that the diffusion coefficients of bulk-water in the protein water system is very similar to the respective experimental values and the diffusion behavior of the hydration water is retarded significantly, with a temperature dependent scaling. At low temperatures, the scaling effects are larger than at higher temperatures for both the proteins; For example, using a cutoff value of 3.4 Å, the hydration water diffusion is scaled by 48-54 % with respect to the bulk water at lower temperatures (273 K), and between 37-43 % at higher temperatures (303 K). At a cutoff value of 5.0 Å, the scaling is 35-38% in the low temperature region (273K) and 23-30% at the high temperature region (303K). Within the cutoff radius of 5 Å includes waters in contact with nonpolar heavy atoms, such as methyl groups. These interactions are weaker than the polar interactions observed within the 3.4 Å cutoffs and allow the water to diffuse away from the protein more easily. As the water molecules are sampled at a higher cutoff value, farther away from the protein surface the results consistently show that the hydration water molecules progressively tend to attain the characteristics of the bulk water behavior. Although the actual scaling at each temperature for CPI and Ovomucoid is different, the rate of scaling obtained

using the linear fit with respect to (T/η) is similar, for both the scaling factors. The variation of D_S values with respect to (T/η) is analyzed using linear regression methods and the results are summarized in **Table 2**. The temperature dependence of bulk water from the protein water system is very close to that of the experimental values (6.91 $\pm$ 0.06 N/K and 6.37 $\pm$ 0.02 N/K, for CPI and Ovomucoid, respectively), and the experimental bulk water has a slope of 6.64 $\pm$ 0.01 N/K. The rate of change of D_s with T/η shows how closely the simulated values resemble the experimental values. The same metric can also be used as a measure to compare the diffusion characteristics between the surface and bulk waters in the protein-water system. Overall, the temperature dependence of the translation diffusion of bulk water from the simulations is in reasonable agreement of the simulations to experiments. Comparison of the calculated diffusion coefficients between the bulk and hydration water molecules (Figure 3 and Table 2) shows the protein induced rate change of solvent translational diffusion coefficient with respect to T/η is ~30% at a cutoff 3.4 Å (26.9 % and 33.3 % for CPI and Ovomucoid, respectively) ~18% at a cutoff 5.0Å (16.9% and 19.9 for CPI and Ovomucoid, respectively) over the temperature range studied.

Influence of polar and nonpolar residues on water diffusion.

Interaction between the protein and water molecules is not uniform at the surface and it is largely determined by the nature of the surface exposed amino acids. **Table 3** lists the diffusion coefficient of water molecules (calculated at a cutoff of 3.4 Å) close to the surface polar and nonpolar residues. In general the diffusion constant of water molecules close to the polar residues are slightly higher than the nonpolar ones. The difference in the diffusion constants are in the range of 0.1 to 0.3 (10^{-9} m^2s^{-1}) and these differences are tend to be slightly larger for CPI than for Ovomucoid. The temperature dependence on the influences of diffusion coefficients between polar and nonpolar

residues is complex and can arise from several factors: For example the hydrophobic effect increases with increase in temperature (40,41) reflecting increased disparity between perturbed waters forced to align themselves around nonpolar groups (42) and those free to interact with bulk solvent.

Hydration hydrodynamics

The observed variation in the diffusion coefficient of protein hydration water molecules, from the Stokes-Einstein equation (Eq. [1]) can arise either due to a change in the viscosity (η) or the radius (*a*) or both. Experimental measurement of the bulk water rotational correlation time (τ_s) follows the viscosity over a wide range of temperatures (43) and in fact the observed change in the radius is only 1.7% in the temperature range of –10º to 60°C (44). Therefore, the assumption that modulation of the translational dynamics of hydration water molecules is predominantly due local changes in the viscosity induced by frictional coupling between the protein and surface waters is reasonable.

Hydration hydrodynamics model shows that the frictional coupling between protein and solvent is a major contributing factor for observed changes in protein dynamics (32). In this model, the ratio of the translational diffusion constant of a protein that is perturbed by the solvent (D_P) to the unperturbed (D_P^o) is given by

$$\frac{D_P}{D_P^o} = 1 - (1 - \alpha_T)\left(1 - \frac{\eta_o}{\eta_S}\right) \qquad [2]$$

where η_o and η_s the viscosity of bulk and surface water molecules, respectively and α_T is the geometrical quantity for the translational motion given by

$$\alpha_T = \left(\frac{V_P}{V_P + V_S} \right)^{\frac{1}{3}} \quad [3]$$

where V_P is the volume of the protein immersed inside an incompressible liquid of viscosity η_s within a spherical shell of volume V_S and the bulk value of viscosity η_o everywhere else. When V_S = 0 and/or $\eta_s = \eta_o$, water molecules are not influenced by the protein and conversely the protein dynamics is described by the Stokes-Einstein equation (similar to Eq. [1], but for the proteins). At the other limit when $\eta_s >> \eta_o$, referred to as 'solvent-berg' limit, the protein molecule has the most influence on hydration water molecules and a clear distinction with bulk water is established (32).

Rewriting Eq. [2] in terms of the solvent translation dynamics with the assumption that the radius of the water molecule remains the same between bulk and hydration conditions,

$$\frac{D_S^H}{D_S^o} = 1 - \left(\frac{1}{1 - \alpha_T} \right) \left(1 - \frac{D_P}{D_P^o} \right) \quad [4]$$

Equation [4] shows that the translational dynamics of hydration water is directly related to the dynamic parameters of the protein. Therefore, it is possible to estimate the RHS of Eq. [4] to determine the expected scaling of the hydration waters with respect to bulk water. The two parameters that need to be estimated are α_T and D_P / D_P^o.

Geometrical factor α_T is normally estimated from the three dimensional structural parameters by assuming that the volume of the hydration shell (V_S) is proportional to the protein surface area A_P,

$$V_S = \lambda_S A_P \qquad [5]$$

where the effective shell thickness λ_S, can be assumed to be 2 Å (less than its diameter, 2.8 Å)(32). **Table 4** lists the molecular properties for CPI and Ovomucoid, including surface area, molecular volume, and Stokes volume along with the estimated α_T values. Using the molecular surface area of CPI and Ovomucoid estimated from their 3D structures (Table 4), the average value for α_T becomes 0.76. As a comparison, the geometrical factor estimated for rotational contribution is 0.56 and the corresponding translational value is 0.82 ($\alpha_T = \sqrt[3]{\alpha_R}$) for lysozyme. Alternatively, we have calculated the geometrical factor, where V_S in Eq. [5] is assumed to be equal to the corresponding Stokes volume (Table 4) of the protein. This procedure resulted in slightly smaller values of α_T ~0.71 for both proteins than the first procedure.

In order to determine the second ratio (D_P / D_P^o), D_P^o diffusion constant of the non-hydrated protein is traditionally estimated from Eq.[1], where the effective radius is determined from the volume estimated by $V_P = M_P \bar{\nu}_P$, where M_P is the molecular weight and $\bar{\nu}_P$ is the partial specific volume (0.073 m^3kg^{-1}). To account for the temperature dependence of D_P values, we calculated the translational diffusion constant of the proteins as a function of the hydration-scaling factor (variable effective atomic radius) and the results are extrapolated to no-hydration to determine D_P^o (D_P solvent unperturbed diffusion). **Figure S1** (supporting information) shows the plot of the calculated self-diffusion coefficient for CPI and Ovomucoid as a function of the scaling factor (see materials and methods) and averaged over the range of temperatures simulated (273-303 K) along with the linear regression (continuous lines) and

confidence interval at 95% (dotted lines). The intercept that corresponds to D_P^o is estimated to be 16.4 $\times 10^{-10}$ $m^{-2}s^{-1}$ (m^2s^{-1}) and 14.4 $\times 10^{-10}$ $m^{-2}s^{-1}$ (m^2s^{-1}), for CPI and Ovomucoid respectively (Table 2). Estimation of D_P is approximate as the exact nature of the hydration depends critically on the surface composition. Comparison of the rotational correlation times of proteins determined using NMR based relaxation methods(45,46) suggest that scaling factors typically vary between 2.8 Å and 3.8 Å, with the distribution centered at 3.3 Å. Therefore when using a hydration scaling radius of 3.3 Å to estimate D_P, the hydration hydrodynamics theory predicts a reduction in the translational diffusion coefficient of hydration water between 39-82% (39-75% for CPI and 41-84% for Ovomucoid), with respect to the bulk water over the temperature range simulated. In comparison, MD simulations (Table 1) estimate a reduction of 35-52 % with respect to the bulk water (37-48% for CPI and 43-52% for Ovomucoid). Increasing the cutoff value to determine the hydration water diffusion constants from 3.4 to 5.0 Å (Table 1), this range reduces to 23-38%. This change in the reduction is an outcome of the fact that at 5.0 Å cutoff, the protein surface has less influence on the hydration waters and adopts more 'bulk-like' behavior. Although the hydration hydrodynamics based prediction do not match with the MD simulations perfectly, there is a good agreement between the results. For example, using the experimental information on ^{17}O magnetic resonance dispersion studies, Halle and Davidovic (32) adopted an average value of $\left\langle \frac{\tau_0}{\tau_s} \right\rangle$ (ratio of the rotational correlation times of bulk and hydration water) to be 0.35. Indeed, experimental rotational correlation based validation is a better method as it is much more sensitive and localized in comparison with the translational diffusion. It must be emphasized that variations in D_P values estimated from the hydrodynamics calculations are approximate as they do not account for the variation in the temperature and viscosity

explicitly. More importantly, these results do not reflect the finer changes that occur locally on the protein surfaces such as cavities.

Discussion

Water mobility in the proximity of the protein surface exhibits a wide range of dynamical behaviors; from very tightly bound water to highly mobile water molecules. Different categories of water behavior can be characterized depending on their residence times. One type is strongly bound to (in) the protein, which can be identified crystallographically and plays an important role in stabilizing the native structure. The residence time of these water molecules is usually in the range of 10^{-9} to 10^{-3} s. Another type of water is more dynamic (shorter residence times) and is interfacial in nature. The third type of water is in the vicinity of the protein surface but not directly interacting with the protein and displays bulk-like behavior. Our main interest is in the dynamics of the third class of water molecules that predominantly determine the hydration structure on protein surfaces.

The radial distribution functions of water with respect to various protein atomic sites reveal the structural organization of water near the protein surface (8,47). The radial distribution functions around the polar and nonpolar atomic sites have similar distribution between the two proteins studied. The effect of polar vs. nonpolar residue's influence is more clearly seen in the respective water diffusion coefficients (Table 3). Temperature dependence of the hydration hydrodynamics is schematically shown in figure 4. **Figure 4** was generated by placing the protein at the origin at every time step. A 50 $Å^3$ grid with 1 $Å^3$ spacing was used to count up the number density of the oxygen's in water for 1 ns. The top and bottom rows show the results for CPI and Ovomucoid, respectively. With increase in temperature density of water molecules surrounding the protein decreases. It is interesting to note that the change in the density is not uniform around the surface, with concave surfaces on both the proteins continue to maintain a higher density of water molecules even at higher temperatures. Surface shape effects

are not unusual as evidenced by Hua et al., (47) that concave regions have a broader distribution compared to the sites in the convex region. Though the surface composition of the protein affects the hydration dynamics, the proteins themselves do not undergo any large-scale dynamics over the simulation length. For example, the variation in the radius of gyration (Rg) over the last 1ns of the simulation of the protein shows only a little variation comparison with the Rg estimated from their respective X-ray structures (**Table S1**).

Extensive experimental information on the rotational and translational dynamics of bulk water is available. However, characterization of the hydration water is often inferred indirectly from the dynamic parameters of the protein. Experimental values of hydration water determined using magnetic resonance dispersion studies are about 5 times smaller than the bulk water (6) and that by neutron scattering tend to predict much less that factor of 5 (1). Recently, Marchi et al (48), have performed MD simulations of lysozyme at 300K found that hydration water dynamics is scaled between 3-7 times depending on the definition of the hydration shell. Our results are in broad agreement with the magnetic relaxation dispersion studies and other MD simulations in general. We have shown here how the translational dynamics of water molecules can be followed using MD simulations and explained based on hydration hydrodynamics. The exact nature of the mechanism however needs extensive and accurate experimental data on the global translational motion of proteins as a function of temperature.

At large distances from the protein surface, as is presented here, the bulk water diffusion results are closely reproduced by simulation. However, the simulation results on the surface water molecules tend to be more inconsistent (5). In addition to the current results, several important observations were made and these can be classified into three major classes; (a) anisotropic diffusion of water on the protein surface (5,49),

(b) anomalous diffusion of the water that introduces a non-linear behavior to the Stokes-Einstein equation to describe the water diffusion in the presence of proteins (50-52) and (c) apparent increase in the density of water molecules close to the protein surface (20,53-55). How each of these earlier observed protein surface induced effects on the translational behavior of the hydration water molecules needs much more elaborate study than what is presented here. Our goal was to first determine the temperature dependence of the hydration waters in proteins and then to determine how the simulations relate to hydration hydrodynamics theory. The agreement between the simulations and the theory is modest and most of the discrepancy between them can be traced to a large extent to the estimation of D_P.

Conclusions

Water plays a primary role in the flexibility of proteins and is critical to the conformational changes required for enzymatic activity (9). The frictional coupling between protein motions and water dynamics has been suggested that fluctuations of the hydration water can slave the protein dynamics and thus affect its function (29,56,57). The interplay between the protein and solvent complexity has several intriguing open questions, for example how much water (quantity) is affected by the presence of the protein. Most x-ray crystallographic studies have suggested that only the first solvent layer is affected, whereas calorimetric studies suggest that more than one layer is affected. Recently, Bano and Marek (58) have investigated the volume properties of protein hydration layers by Monte Carlo modeling. The thickness of the thermal volume layer as calculated in their framework of the scaled particle theory is 0.6-0.65 Å. This value is significantly lower than ones presented for proteins in earlier papers (where proportionality between the hydration level and the area of charged and polar surfaces was assumed), but is close to the value published for small solute molecules. At the other extreme, certain glycoproteins tend be much more hydrated than most globular proteins and a scaling factor of > 5.5 Å is required to fit the temperature dependent translational diffusion coefficient. These differences in hydration properties could be natural to the protein and its function, in particular for proteins that function at extreme environments such as thermophilic or antifreeze proteins. We expect that new experimental approaches to measure the dynamic properties of the hydration layer and improved simulation methods will shed additional information. Our results provide one of the necessary steps that will lead to a comprehensive understanding of the role of hydration hydrodynamics in proteins structure, dynamics, as well as function.

Materials and Methods

Molecular Dynamics Simulations

All molecular dynamics simulations were performed with Amber 7 (59) using the Cornell force field (60). The proteins were chosen because of their small size and can be simulated with an overall neutral charge, thus no counterions are necessary. The carboxypeptidase inhibitor (RCSB ID, 1H20, first 37 residues) (61) and ovomucoid (RCSB ID, 2OVO) (62) were prepared in the following manner. The proteins were solvated in boxes of SPC/E (63) water sufficient to have 15 Å of water between the protein and the interface. SPC/E water was chosen because of its well-characterized behavior over a large range of temperatures (64). The system was energy minimized using a combination of steepest descents and conjugate gradient methods. Constant pressure, constant temperature molecular dynamics (65) was performed on the energy minimized system to randomize the water and to adjust the water density. A time step of 1 fs was used and the SHAKE algorithm was used to constrain bonds containing hydrogen (66). The system was coupled to a heat bath at 303 K. Particle mesh Ewald summation was used to treat the long range interactions using a 9 Å cutoff in direct space with an 1 Å grid (67). The NPT simulations for the caroboxypeptidase inhibitor and ovomucoid were performed for 200 ps.

The final structure from the NPT simulation was energy minimized. This energy-minimized structure was used as the starting structure for all the NVE simulations and the box size was adjusted to have the appropriate density at the given temperature. All the NVE simulations started at 0 K and the velocities on the atoms were reassigned until they were at the appropriate temperature. All other aspects of the simulations were the same as stated above. Each simulation at a given temperature was run for a total of 2 ns with the last 1 ns were used for analysis.

The mean squared displacements (MSD) for bulk solvent were calculated in 100 ps windows and averaged. Diffusion constants for the bulk solvent were estimated from the slope of the MSD and multiplied by 5/3 to obtain the correct units (The mean squared displacement plotted against time for the simulation data gives a slope in $Å^2$/ps. To convert to the appropriate units for a diffusion constant we get cm^2/s(*10) and divide by 6 (for the degrees of freedom)). Hydration water was defined using two independent values, within 3.4 Å of a heavy protein atom and 5.0 Å of a heavy protein atom. Inspection of the MSD for the hydration waters over 100 ps shows two regimes. The MSD is linear to approximately 50 ps at the different temperatures but after 50 ps, the slope of the MSD increases (likely showing the hydration water exchanging to the bulk). The diffusion constants for the hydration waters were estimated with 50 ps windows and averaged.

Protein Hydrodynamic Calculations

Translational diffusion tensor values were calculated based on the beads model approximation of García de la Torre and Bloomfield (68). This method has been used successfully to calculate translational as well as rotational diffusion tensors of proteins (46,69-73). In this method, the protein is modeled as a collection of point sources of friction (denoted as beads) with hydrodynamic tensor interactions between them. The rotational diffusion tensor is calculated from a set of linear equations solved by integrating a $3N \times 3N$ matrix, where N is the number of atoms determined from the structure of the protein. The program DIFFC, based on the beads theory (73), was used in the present work. All atoms were considered as beads of equal size for a range of different values (σ = 1.5 to 5.5 in steps of 1Å, and at 7 temperature values ranging from 273 K to 303 K) for purposes of calculating the diffusion tensor as a function of temperature. Experimental values of the viscosity (in Nsm^{-2}) of pure water (74) were

used. The overall isotropic translational self-diffusion coefficient was calculated by taking the average of the principal values of the diffusion tensor.

Acknowledgements

Thanks to Drs. S. Mielke and Professor Y.Duan for critical reading of the manuscript. This work was sponsored by the U.S. Department of Energy, Office of Science, This work was in part (for EYL) performed under the auspices of the United States Department of Energy by the University of California, Lawrence Livermore National Laboratory under contract number W-7405-ENG-48.

Figure Captions

Figure 1: Uncorrected water-protein radial distribution functions around equilibrated CPI, nonpolar (left panels) and polar (right panels) as a function of the distance between backbone α-carbon (a and d), carbonyl (b and e) and nitrogen (c and f) atoms to the water oxygen atom. Three representative temperatures at 273, 288 and 303K were shown as continuous (black), long-dashed (red) and dashed (green) lines.

Figure 2: Uncorrected water-protein radial distribution functions around equilibrated Ovomucoid, nonpolar (left panels) and polar (right panels) as a function of the distance between backbone α-carbon (a and d), carbonyl (b and e) and nitrogen (c and f) atoms to the water oxygen atom. Three representative temperatures at 273, 288 and 303K were shown as continuous (black), long-dashed (red) and dashed (green) lines.

Figure 3: Plot of D_s versus T/η for the various water molecules for (a) CPI and (b) Ovomucoid. Experimentally determined bulk water (open circles), bulk water molecules in the simulation (filled circles) and hydration (surface) water molecules on the protein (triangles and filled squares) are shown. The hydration water diffusion with a cutoff of 3.4 Å and 5.0Å were shown as triangles and squares, respectively for each protein. The experimental bulk water diffusion values are same in both (a) and (b), while the simulated values are calculated separately for CPI and Ovomucoid. The straight lines are the linear fit and the dotted lines correspond to the respective 95% confidence limits, confidence limits for the experimental values are not plotted.

Figure 4: Schematic representation of hydration hydrodynamics effects for CPI and Ovomucoid at the top and bottom respectively. The top row shows cartoon views of CPI at 273, 288 and 303 K, respectively where the grids represent density of water

molecules surrounding the protein and bottom row show a similar representation for OVO.

Table

Table 1: Translational diffusion constants of the bulk and hydration waters

Temperature (K)	Translational Diffusion Constant ($\times 10^{-9}$ m^2s^{-1})										
	Experimental [(a)]	CPI					Ovomucoid				
	Bulk water	Bulk water (D_S^o)	Hydration water (D_S^H)		ΔD_S (%)		Bulk water (D_S^o)	Hydration water (D_S^H)		ΔD_S (%)	
			3.4Å	5.0 Å	3.4 Å	5.0 Å		3.4Å	5.0 Å	3.4 Å	5.0 Å
273	1.10	1.31	0.68	0.84	48.1	35.9	1.30	0.62	0.80	52.3	38.7
278	1.30	1.53	0.82	0.99	46.4	35.6	1.57	0.78	1.01	50.3	36.0
283	1.53	1.76	0.99	1.20	43.8	31.8	1.78	0.94	1.15	47.2	35.6
288	1.77	1.97	1.16	1.39	41.1	29.6	1.96	1.08	1.36	44.9	30.5
293	2.02	2.24	1.34	1.51	40.2	32.5	2.25	1.21	1.52	46.2	32.5
298	2.30	2.52	1.57	1.75	37.7	30.7	2.42	1.42	1.73	41.3	28.4
303	2.59	2.84	1.78	2.17	37.3	23.5	2.75	1.55	1.93	43.6	30.0

[(a)] Experimental values were obtained from (75).

Table 2: Linear regression analysis of the temperature dependence of hydration waters.

System	Bulk water			Hydration water		
	Intercept	Slope	CC	Intercept	Slope	CC
Experimental	0.14 ±0.01	6.64 ±0.01	> 0.99			
CPI-water (3.4Å)	0.28 ±0.01	6.91 ±0.06	> 0.99	-0.08 ±0.01	5.05 ±0.04	> 0.99
(5.0Å)				-0.04 ±0.01	5.74 ±0.04	> 0.99
Ovomucoid-water (3.4Å)	0.39 ±0.05	6.37 ±0.02	> 0.99	0.03 ±0.01	4.24 ±0.1	> 0.99
(5.0Å)				-0.07 ±0.03	5.1 ±0.01	> 0.99

CC: Correlation coefficient

Table 3: Diffusion coefficients of water molecules at the polar and nonpolar surface residues.

Temperate (K)	[a]Translational Diffusion Constant ($\times 10^{-9}$ m^2s^{-1})			
	Ovomucoid		CPI	
	Polar Residues	Nonpolar Residues	Polar Residues	Nonpolar Residues
273	0.61	0.47	0.68	0.51
278	0.80	0.66	0.86	0.65
283	0.96	0.83	1.02	0.81
288	1.05	1.00	1.21	0.97
293	1.20	1.08	1.36	1.14
293	1.39	1.33	1.66	1.23
303	1.52	1.43	1.88	1.44

[a] Diffusion coefficients are calculated at a cutoff value of 3.4Å

Table 4: Estimation of Diffusion scaling of water due to hydration

Protein	MW (kD)	Surface Area (Å^2)	Molecular Volume (Å^3)	Stokes Volume (Å^3)	α_T	D_P^o	Hydrodynamic Scale (Å)	D_P^H	ΔD_S (%)
CPI (1H20)	4.28	2776.40	4364.20	7494.53	0.71	16.4	2.0- 4.0	14.49-12.74	39-75
OVO (2OVO)	6.02	3973.20	6486.00	11056.37	0.72	14.4	2.0- 4.0	12.75-11.06	41-82

D_P and D_P are solvent and unperturbed translational diffusion constants, respectively and α_T is defined in Eq.[3].

Table S1: Radius of gyration during the dynamic simulation

Temperature (K)	Ovomucoid Rg (Å)	CPI Rg (Å)
X-ray structure	10.17	8.11
273	10.36 ± 0.12	8.32 ± 0.08
278	10.35 ± 0.13	8.31 ± 0.06
283	10.24 ± 0.13	8.3 ± 0.1
288	10.31 ± 0.12	8.36 ± 0.05
293	10.2 ± 0.12	8.35 ± 0.07
298	10.2 ± 0.13	8.31 ± 0.14
303	10.44 ± 0.09	8.38 ± 0.07

[a] Radius of gyration (using CA for calculation) for proteins was calculated during the last 1ns of the simulation.

References

(1) M Ferrand, A Dianoux, W Petry, G Zaccail: Thermal motions and function of bacteriorhodopsin in purple membranes- Effecrs of temperature and hydration studied by neutron-scattering. Proceedings of the National Academy of Sciences of the United States of America 90 (1993) 9668-72.

(2) HX Zhou: A unified picture of protein hydration: prediction of hydrodynamic properties from known structures. Biophysical Chemistry 93 (2001) 171-79.

(3) RH Henchman, JA McCammon: Structural and dynamic properties of water around acetylcholinesterase. Protein Science 11 (2002) 2080-90.

(4) JC Smith, F Merzel, CS Verma, S Fischer: Protein hydration water: Structure and thermodynamics. Journal of Molecular Liquids 101 (2002) 27-33.

(5) A Bizzarri, S Cannistraro: Molecular dynamics of water at the protein-solvent interface. Journal of Physical Chemistry B 106 (2002) 6617-33.

(6) B Halle: Protein hydration dynamics in solution: a critical survey. Philos Trans R Soc Lond B Biol Sci 359 (2004) 1207-23; discussion 23-4, 323-8.

(7) B Bagchi: Water dynamics in the hydration layer around proteins and micelles. Chemical Reviews 105 (2005) 3197-219.

(8) TM Raschke: Water structure and interactions with protein surfaces. Curr Opin Struct Biol 16 (2006) 1-8.

(9) Y Levy, JN Onuchic: Water Mediation in Protein Folding and Molecular Recognition. Annu Rev Biophys Biomol Struct 35 (2006) 389-415.

(10) S Bone, R Pethig: Dielectric studies of protein hydration and hydration-induced flexibility. Journal of Molecular Biology 181 (1985) 323-26.

(11) U Langhorst, R Loris, V Denisov, J Doumen, P Roose, D Maes, B Halle, J Steyaert: Dissection of the structural and functional role of a conserved hydration site in RNase T1. Protein Science 8 (1999) 722-30.

(12) K Venu, L Svensson, B Halle: Orientational order and dynamics of hydration water in a single crystal of bovine pancreatic trypsin inhibitor. Biophysical Journal 77 (1999) 1074-85.

(13) V Lounnas, S Ludemann, R Wade: Towards molecular dynamics simulation of large proteins with a hydration shell at constant pressure. Biophysical Chemistry 78 (1999) 157-82.

(14) R Jaenicke, H Lilie: Folding and association of oligomeric and multimeric proteins. Advances in Protein Chemistry 53 (2000) 329-+.

(15) A Royant, K Edman, T Ursby, E Pebay-Peyroula, E Landau, R Neutze: Helix deformation is coupled to vectorial proton transport in the photocycle of bacteriorhodopsin. Nature 406 (2000) 645-48.

(16) J Rupley, G Careri: Protein hydration and function. Advances in Protein Chemistry 41 (1991) 37-172.

(17) G Otting, E Liepinsh, K Wuthrich: Protein hydration in aqueous solution. Science 254 (1991) 974-80.

(18) VP Denisov, B Halle: Protein hydration dynamics in aqueous solution: a comparison of bovine pancreatic trypsin inhibitor and ubiquitin by oxygen-17 spin relaxation dispersion. J Mol Biol 245 (1995) 682-97.

(19) B Halle, VP Denisov: A new view of water dynamics in immobilized proteins. Biophys J 69 (1995) 242-9.

(20) DI Svergun, S Richard, MH Koch, Z Sayers, S Kuprin, G Zaccai: Protein hydration in solution: experimental observation by x-ray and neutron scattering. Proc Natl Acad Sci U S A 95 (1998) 2267-72.

(21) J Badger, DL Caspar: Water structure in cubic insulin crystals. Proc Natl Acad Sci U S A 88 (1991) 622-6.

(22) MM Teeter, SM Roe, NH Heo: Atomic resolution (0.83 A) crystal structure of the hydrophobic protein crambin at 130 K. J Mol Biol 230 (1993) 292-311.

(23) FT Burling, WI Weis, KM Flaherty, AT Brunger: Direct observation of protein solvation and discrete disorder with experimental crystallographic phases. Science 271 (1996) 72-7.

(24) AD Podjarny, EI Howard, A Urzhumtsev, JR Grigera: A multicopy modeling of the water distribution in macromolecular crystals. Proteins 28 (1997) 303-12.

(25) BP Schoenborn, A Garcia, R Knott: Hydration in protein crystallography. Prog Biophys Mol Biol 64 (1995) 105-19.

(26) N Niimura, Y Minezaki, T Nonaka, JC Castagna, F Cipriani, P Hoghoj, MS Lehmann, C Wilkinson: Neutron Laue diffractometry with an imaging plate provides an effective data collection regime for neutron protein crystallography. Nat Struct Biol 4 (1997) 909-14.

(27) F Shu, V Ramakrishnan, BP Schoenborn: Enhanced visibility of hydrogen atoms by neutron crystallography on fully deuterated myoglobin. Proc Natl Acad Sci U S A 97 (2000) 3872-7.

(28) V Makarov, B Andrews, P Smith, B Pettitt: Residence times of water molecules in the hydration sites of myoglobin. Biophysical Journal 79 (2000) 2966-74.

(29) V Makarov, B Pettitt, M Feig: Solvation and hydration of proteins and mucleic acids: A theoretical view of simulation and experiment. Accounts in Chemical Research 35 (2002) 376-84.

(30) B Pettitt, V Makarov, B Andrews: Protein hydration density: theory, simulations and crystallography. Current Opinion in Structural Biology 8 (1998) 218-21.

(31) C Gonzalez, JL Neira, S Ventura, S Bronsoms, M Rico, FX Aviles: Structure and dynamics of the potato carboxypeptidase inhibitor by 1H and 15N NMR. Proteins 50 (2003) 410-22.

(32) B Halle, M Davidovic: Biomolecular hydration: from water dynamics to hydrodynamics. Proc Natl Acad Sci U S A 100 (2003) 12135-40.

(33) M Levitt, R Sharon: Accurate simulation of protein dynamucs in solution. Proceedings of the National Academy of Sciences of the United States of America 85 (1988) 7557-61.

(34) G Phillips, B Pettitt: Structure and dynamics of the water around myoglobin. Protein Science 4 (1995) 149-58.

(35) W Gu, BP Schoenborn: Molecular dynamics simulation of hydration in myoglobin. Proteins 22 (1995) 20-6.

(36) A Einstein: Investigations on the theory of Brownian movement, Dover, New York, 1956.

(37) L Landau, D, EM Lifshitz: Fluid Mechanics, Pergamon, Oxford, 1959.

(38) AA Miller: Glass-transition temperature of water. Science 163 (1969) 1325-26.

(39) WS Price, H Ide, Y Arata: Self-diffusion of supercooled water to 238 K using PGSE NMR diffusion measurements. Journal of Physical Chemistry a 103 (1999) 448-50.

(40) W Kauzmann: Some factors in the interpretation of protein denaturation. Adv Protein Chem 14 (1959) 1-63.

(41) C Tanford, PK De: The unfolding of beta-lactoglobulin at pH 3 by urea, formamide, and other organic substances. J Biol Chem 236 (1961) 1711-5.

(42) C Tanford: Protein denaturation. Adv Protein Chem 23 (1968) 121-282.

(43) K Modig, B Halle: Proton magnetic shielding tensor in liquid water. J Am Chem Soc 124 (2002) 12031-41.

(44) P Balbuena, K Johnston, P Rossky, J Hyun: Aqueous ion transport properties and water reorientation dynamics from ambient to supercritical conditions. Journal of Physical Chemistry B 102 (1998) 3806-14.

(45) P Bernado, J Garcia de la Torre, M Pons: Interpretation of 15N NMR relaxation data of globular proteins using hydrodynamic calculations with HYDRONMR. J Biomol NMR 23 (2002) 139-50.

(46) VV Krishnan, M Cosman: An empirical relationship between rotational correlation time and solvent accessible surface area. Journal of Biomolecular NMR 12 (1998) 177-82.

(47) L Hua, XH Huang, RH Zhou, BJ Berne: Dynamics of water confined in the interdomain region of a multidomain protein. Journal of Physical Chemistry B 110 (2006) 3704-11.

(48) M Marchi, F Sterpone, M Ceccarelli: Water rotational relaxation and diffusion in hydrated lysozyme. J Am Chem Soc 124 (2002) 6787-91.

(49) P Ahlstrom, O Teleman, B Jonsson: Molecular dynamucs simulation of interfacial water structure and dynamics in parvalbumin solution. Journal of American Chemical Society 110 (1988) 4198-203.

(50) A Bizzarri, S Cannistraro: Molecular dynamics simulation evidence of anomalous diffusion of protein hydration water. Physical Review E 53 (1996) R3040-R43.

(51) A Bizzarri, C Rocchi, S Cannistraro: Origin of the anomalous diffusion observed by MD simulation at the protein-water interface. Chemical Physics Letters 263 (1996) 559-66.

(52) AR Bizzarri, S Cannistraro: Molecular dynamics simulation evidence of anomalous diffusion of protein hydration water. Physical Review. E. Statistical Physics, Plasmas, Fluids, And Related Interdisciplinary Topics 53 (1996) R3040-R43.

(53) F Merzel, JC Smith: High-density hydration layer of lysozymes: molecular dynamics decomposition of solution scattering data. J Chem Inf Model 45 (2005) 1593-9.

(54) F Merzel, JC Smith: Is the first hydration shell of lysozyme of higher density than bulk water? Proceedings of the National Academy of Sciences of the United States of America 99 (2002) 5378-83.

(55) JC Smith, F Merzel, AN Bondar, A Tournier, S Fischer: Structure, dynamics and reactions of protein hydration water. Philos Trans R Soc Lond B Biol Sci 359 (2004) 1181-9; discussion 89-90.

(56) A Ansari, CM Jones, ER Henry, J Hofrichter, WA Eaton: The role of solvent viscosity in the dynamics of protein conformational changes. Science 256 (1992) 1796-8.

(57) PW Fenimore, H Frauenfelder, BH McMahon, FG Parak: Slaving: solvent fluctuations dominate protein dynamics and functions. Proc Natl Acad Sci U S A 99 (2002) 16047-51.

(58) M Bano, J Marek: How thick is the layer of thermal volume surrounding the protein? Biophys Chem 120 (2006) 44-54.

(59) DA Pearlman, Case, D. A., Caldwell, J. W., Ross, W. S., Cheatham, T. E., III, Debolt, S., Ferguson, D., Seibel, G., and Kollman, P. A.: AMBER, A Package of Computer Programs for Applying Molecular Mechanics, Normal-Mode Analysis, Molecular Dynamics, and Free Energy Calculations to Simulate the Structural and Energetic Properties of Molecules. Comput. Phys. Commun. 91 (1995) 1-41.

(60) WD Cornell, Cieplak, P., Bayly, C. I., Gould, I. R., Merz, K. M., Ferguson, D. M., Spellmeyer, D. C., Fox, T., Caldwell, J. W., and Kollman, P. A.: A 2nd Generation Force Field for the Simulation of Protein, Nucleic Acids, and Organic Molecules. J. Am. Chem. Soc. 117 (1995) 5179-97.

(61) C Gonzalez, Neira, J. L., Ventura, S., Bronsoms, S., Rico, M., Aviles, X.: Structure and Dynamics of the Potato Carboxypeptidase Inhibitor by 1H and 15N NMR. Proteins: Struct., Funct., Genet. 50 (2003) 410-22.

(62) W Bode, Epp, O., Huber, R., Laskowski, M., Ardelt, W.: The Crystal and Molecular Structure of the Third Domain of Silver Pheasant Ovomucoid (OMSVP3). Euro. J. Biochem. 147 (1985) 387-95.

(63) HJC Berendsen, Grigera, J. R., Straatsma, T. P.: The Missing Term in Effective Pair Potential. J. Phys. Chem. 91 (1987) 6269-71.

(64) S Harrington, Poole, P. H., Sciortion, F., Stanley, H. E.: Equation of State of Supercooled Water Simulated using the Extended Simple Point Charge Intermolecular Potential. J. Chem. Phys. 107 (1997) 7443-50.

(65) HJC Berendsen, Postma, J. P. M., van Gunsteren, W. F., DiNola, A., Haak, J. R.: Molecular Dynamics with Coupling to an External Bath. J. Chem. Phys. 81 (1984) 3684-90.

(66) JP Ryckaert, Ciccotti, G., and Berendsen, H. J. C.: Numerical Integration of the Cartesian Equations of Motion of a System with Constraints: Molecular Dynamics of n-alkanes. J. Comput. Phys. 23 (1977) 327-41.

(67) U Essmann, Perera, L., Berkowitz, M. L., Darden, T., Lee, H., and Pedersen, L. G.: A Smooth Particle Ewald Mesh Method. J. Chem. Phys. 103 (1995) 8577-93.

(68) JG Garcia de la Torre, VA Bloomfield: Hydrodynamic properties of complex, rigid, biological macromolecules: theory and applications. Quarterly Reviews in Biophysics 14 (1981) 81-139.

(69) J Garcia de la Torre, ML Huertas, B Carrasco: Calculation of hydrodynamic properties of globular proteins from their atomic-level structure. Biophys Journal 78 (2000) 719-30.

(70) J Garcia de la Torre, ML Huertas, B Carrasco: HYDRONMR: prediction of NMR relaxation of globular proteins from atomic-level structures and hydrodynamic calculations. Journal of Magnetic Resonance 147 (2000) 138-46.

(71) V Krishnan, R Feeney, W Fink, Y Yeh: Translational dynamics of antifreeze glycoprotein (AFGP) in supercooled water. Biophysical Journal 82 (2002) 310A-10A.

(72) VV Krishnan: Determination of oligomeric state of proteins in solution from pulsed-field-gradient self-diffusion coefficient measurements. A comparison of experimental, theoretical, and hard-sphere approximated values. Journal of Magnetic Resonance 124 (1997) 468-73.

(73) VY Orekhov, DE Nolde, AP Golovanov, DM Korzhnev, AS Arseniev: Processing of Heteronuclear NMR Relaxation Data With the New Software Dasha. Applied Magnetic Resonance 9 (1995) 581-88.

(74) CH Cho, J Urquidi, S Singh, GW Robinson: Thermal offset viscosities of liquid H2O, D2O, and T2O. Journal of Physical Chemistry B 103 (1999) 1991-94.

(75) M Holz, S Heil, A Sacco: Temperature-dependent self-diffusion coefficients of water and six selected molecular liquids for calibration in accurate H-1 NMR PFG measurements. Physical Chemistry Chemical Physics 2 (2000) 4740-42.

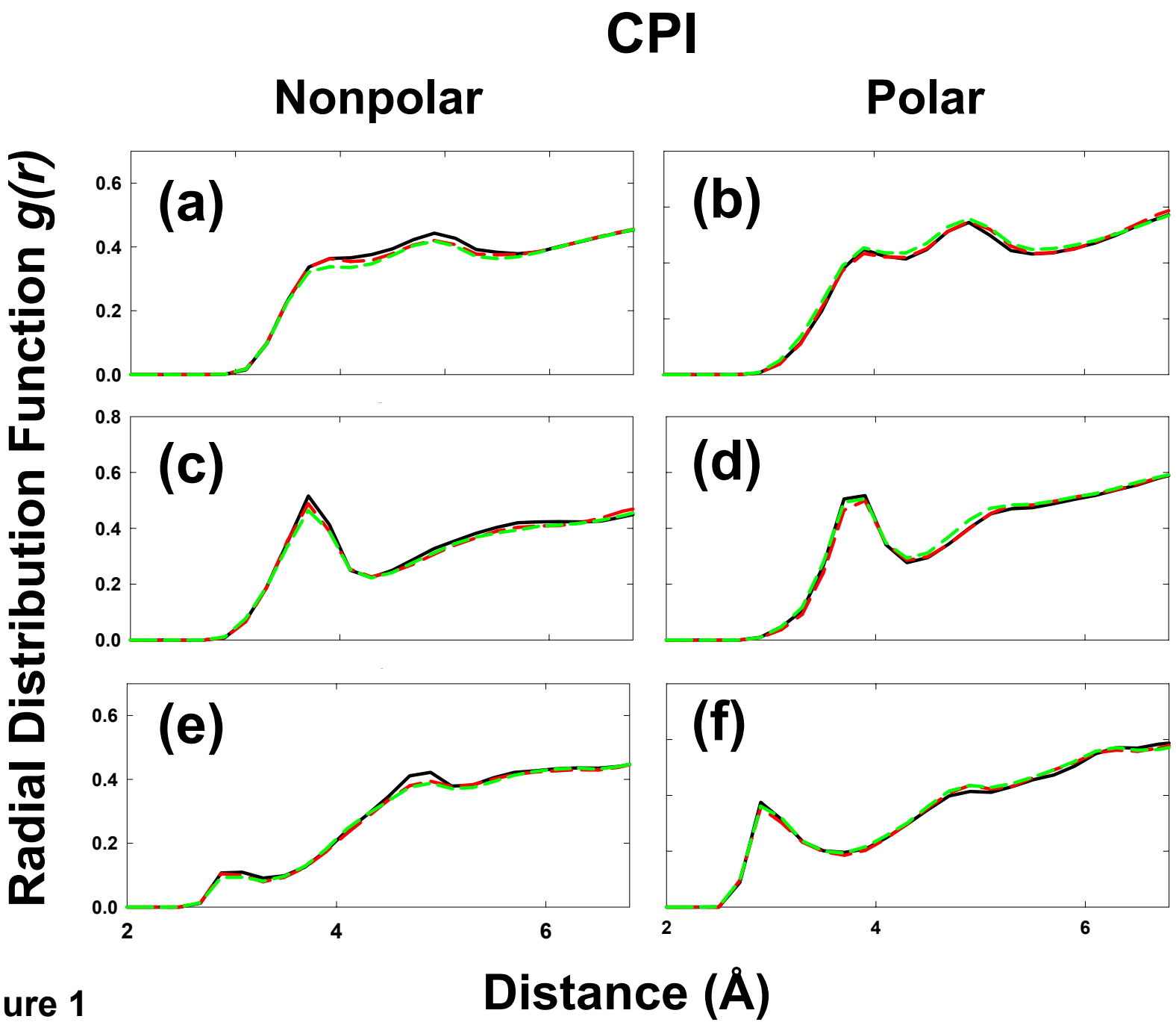
CPI
Nonpolar
Polar
(a)
(b)
(c)
(d)
(e)
(f)
Radial Distribution Function g(r)
Distance (Å)
0.0
0.2
0.4
0.6
0.8
2
4
6

Figure 1

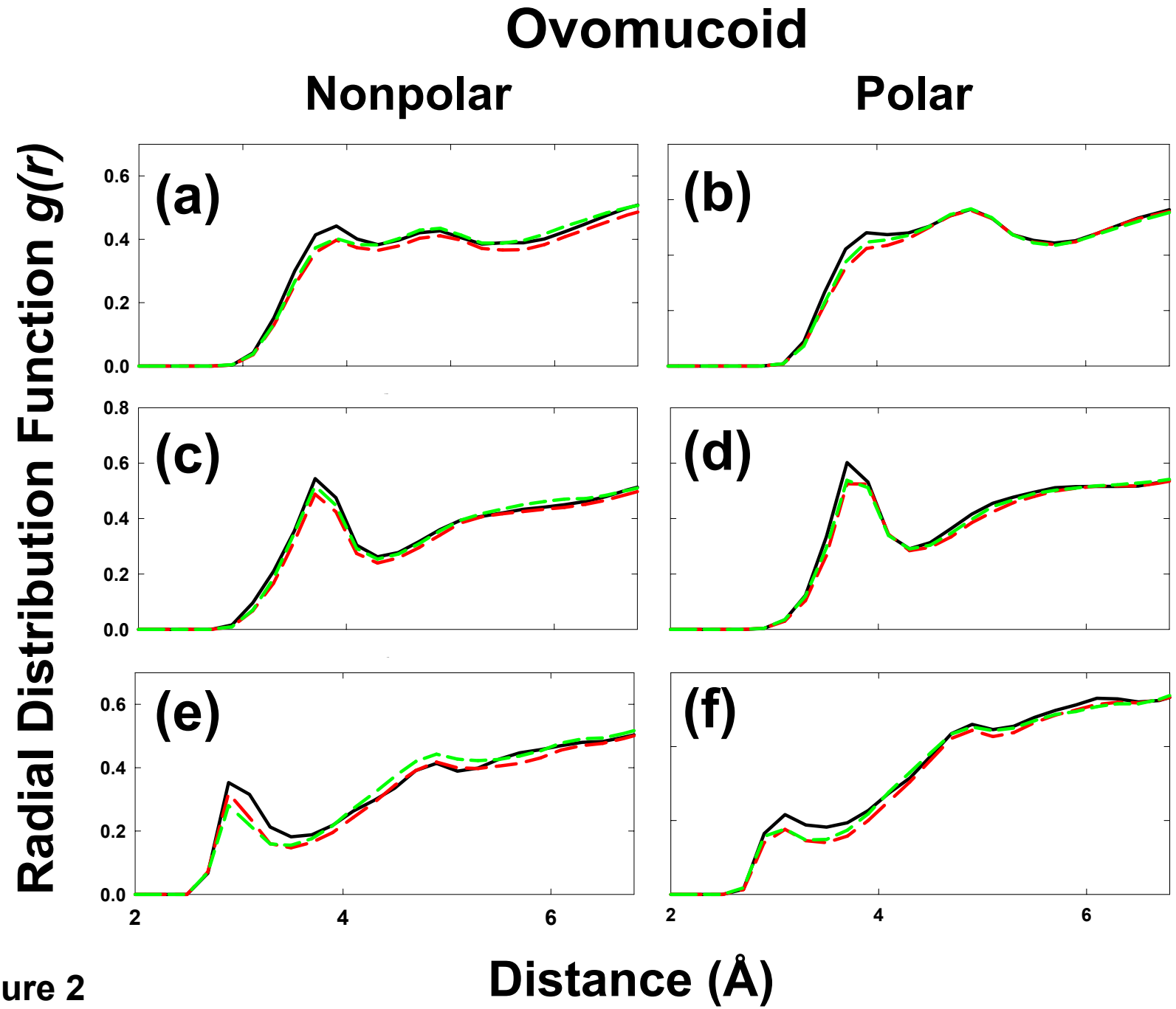
Ovomucoid
Nonpolar
Polar
Radial Distribution Function g(r)
(a)
(b)
(c)
(d)
(e)
(f)
0.0
0.2
0.4
0.6
0.8
2
4
6
Distance (Å)

Figure 2

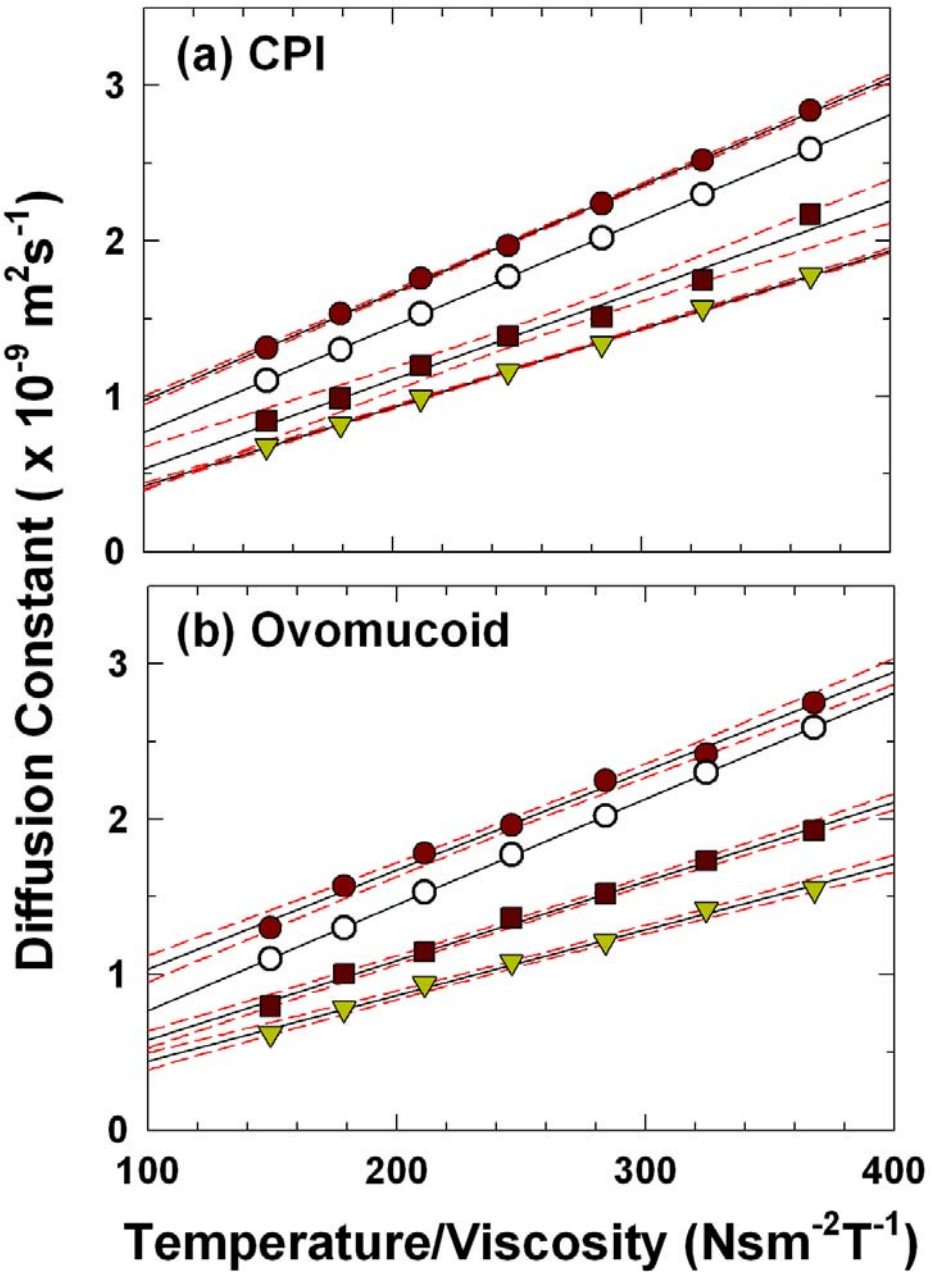
(a) CPI
(b) Ovomucoid
Diffusion Constant (x 10^{-9} m^{2}s^{-1})
Temperature/Viscosity (Nsm^{-2}T^{-1})
0
1
2
3
100
200
300
400

Figure 3

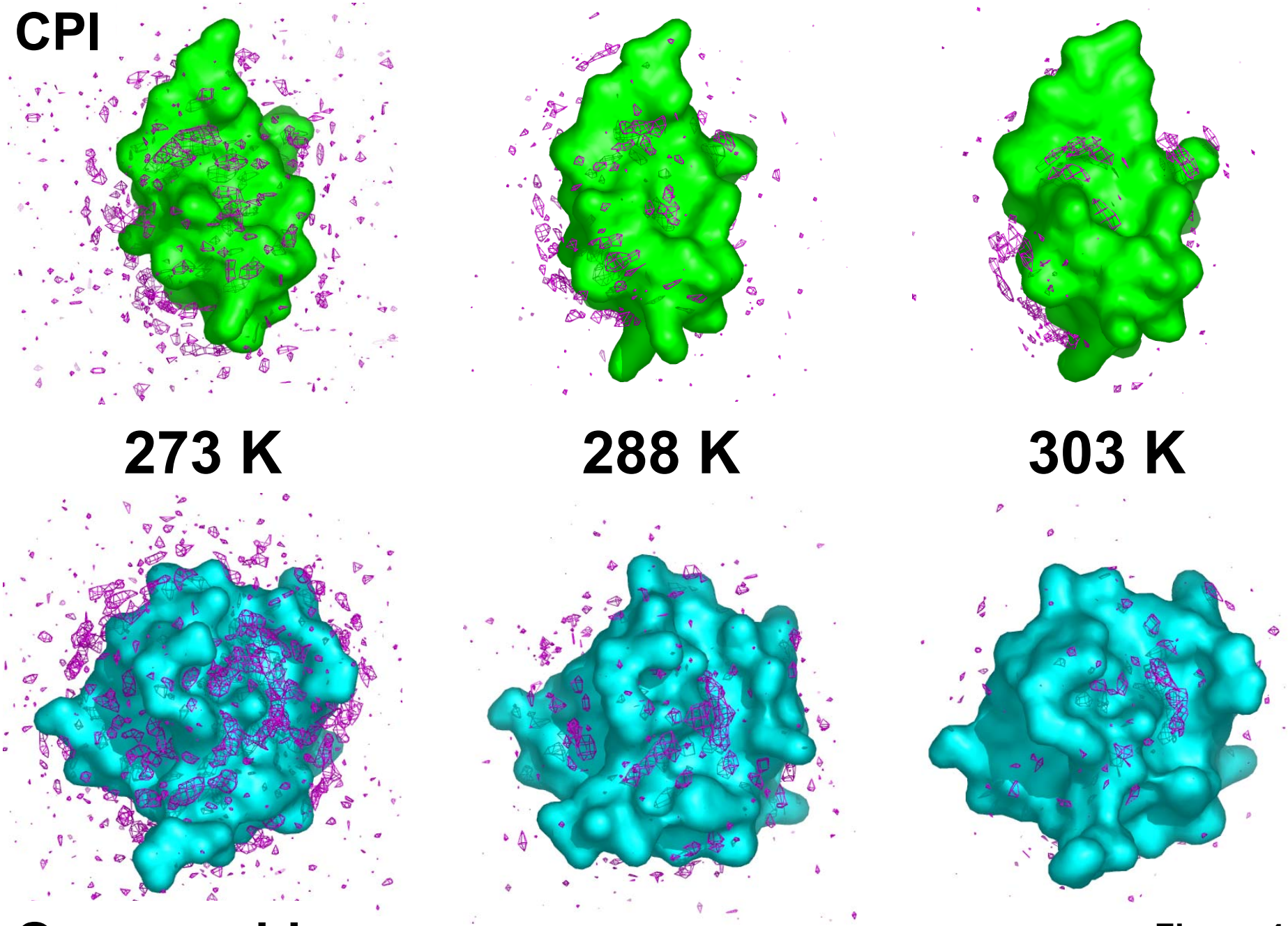

Figure 4

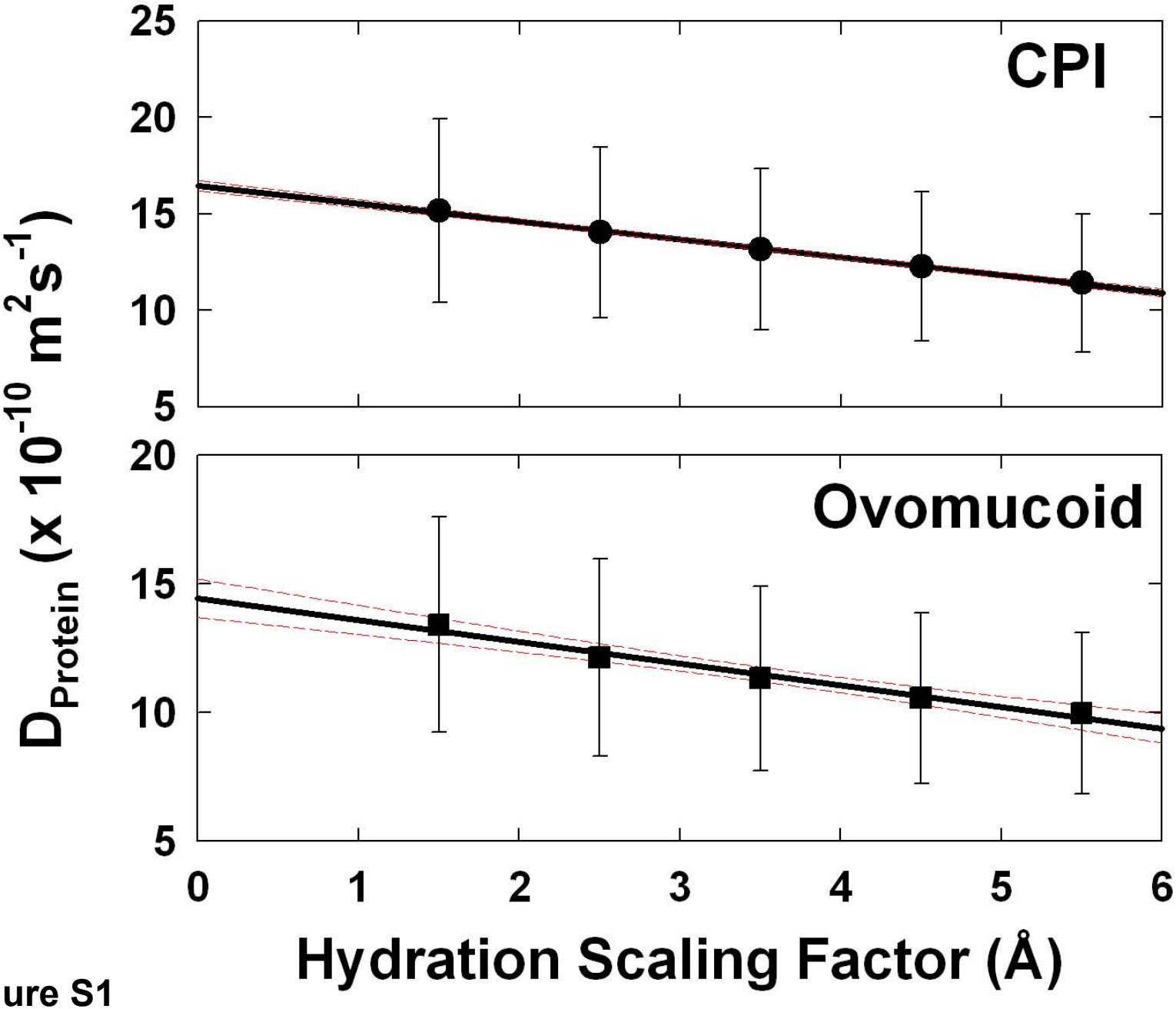
CPI
Ovomucoid
25
20
15
10
5
20
15
10
5
0
1
2
3
4
5
6
$D_{Protein}$ (x 10^{-10} m^2s^{-1})
Hydration Scaling Factor (Å)

Figure S1